四川大学学报（医学版） 2022，53（1）：63－70
J Sichuan Univ（Med Sci）

·论　著·

M2巨噬细胞外泌体对高糖高胰岛素条件下小鼠骨髓间充质干细胞成骨分化的影响*

张　程[1]，包丽荣[1]，杨于桃[1]，王　智[2]，李　燕[1△]

1. 口腔疾病研究国家重点实验室 国家口腔疾病临床医学研究中心 四川大学华西口腔医院（成都 610041）；
2. 中山大学附属口腔医院·中山大学光华口腔医学院 广东省口腔医学重点实验室（广州 510055）

【摘要】 目的　探讨M2巨噬细胞外泌体（M2 macrophage exosomes, M2-exo）对高糖高胰岛素条件下小鼠骨髓间充质干细胞（bone marrow mesenchyml stem cells, BMSCs）成骨分化及Hedgehog信号通路的影响。**方法**　诱导小鼠巨噬细胞系RAW 264.7向M2极化后，提取并鉴定M2-exo，检测BMSCs对外泌体的摄取内吞。将BMSCs分为正常对照组（Control组，使用不含胰岛素、不含M2-exo，且葡萄糖浓度为5.5 mmol/L成骨诱导培养基）、高糖高胰岛素组（HGI组，使用含25 mmol/L葡萄糖及174 nmol/L胰岛素的成骨诱导培养基）及高糖高胰岛素M2-exo干预组（HGI+M2-exo组，使用与HGI组相同的培养基，并分别添加6、30、60 μg/mL的M2-exo），成骨诱导7 d后行碱性磷酸酶（alkaline phosphatase, ALP）染色，成骨诱导14 d后行茜素红染色，评估各组BMSCs成骨分化能力。另取Control组、HGI组、HGI+30 μg/mL M2-exo组BMSCs细胞，成骨诱导培养14 d后（qPCR）及成骨诱导21 d后（Western blot）检测成骨及Hedgehog信号通路相关基因及蛋白的表达。**结果**　成功诱导M2巨噬细胞极化，M2极化表面标志物CD206呈强阳性表达。M2-exo呈典型的类圆形双层膜性囊泡结构，粒径主要分布于50～125 nm之间（占总粒子数的99.14%），外泌体标志蛋白CD9、CD63和CD81呈阳性表达。免疫荧光显示M2-exo可被小鼠BMSCs摄取内化。成骨诱导7 d后，HGI组BMSCs的ALP活性低于Control组，经6 μg/mL、30 μg/mL及60 μg/mL的M2-exo干预后，HGI+M2-exo组ALP活性有所逆转，与HGI组相比差异有统计学意义（$P<0.05$）；成骨诱导14 d后，HGI组矿化结节数量较Control组减少，仅HGI+30 μg/mL M2-exo组干预后其矿化水平高于HGI组（$P<0.05$）。qPCR结果显示，HGI组成骨分化相关基因*Alp*、*Runx*2、*Ocn*及Hedgehog通路相关基因*Gli*1、*Smo*、*Ptch*1 mRNA水平与Control组相比均有不同程度的降低，而30 μg/mL M2-exo干预可促进这些基因的上调，与HGI组相比差异有统计学意义（$P<0.05$）；Western blot结果显示，HGI组成骨相关蛋白RUNX2、COL1A1及Hedgehog通路蛋白GLI1的表达下调，而经30 μg/mL M2-exo干预可促进COL1A1及GLI1的表达上调，与HGI组相比差异有统计学意义（$P<0.05$）。**结论**　高糖高胰岛素对BMSCs成骨分化具有抑制作用。M2-exo干预后，BMSCs的Hedgehog信号通路激活且成骨分化能力增强，提示M2-exo具有用于糖尿病骨修复的潜力。

【关键词】 M2巨噬细胞　外泌体　骨髓间充质干细胞　糖尿病　Hedgehog信号通路

Role of M2 Macrophage Exosomes in Osteogenic Differentiation of Mouse Bone Marrow Mesenchymal Stem Cells under High-Glucose and High-Insulin

ZHANG Cheng[1], *BAO Li-rong*[1], *YANG Yu-tao*[1], *WANG Zhi*[2], *LI Yan*[1△]. 1. *State Key Laboratory of Oral Disease, National Clinical Research Center for Oral Diseases, West China Hospital of Stomatology, Sichuan University*, Chengdu 610041, China; 2. *Hospital of Stomatology and Guanghua School of Stomatology, Sun Yat-sen University and Guangdong Provincial Key Laboratory of Stomatology*, Guangzhou 510055, China

△ Corresponding author, E-mail: feifeiliyan@163.com

【Abstract】 Objective　To study the role of M2 macrophage-derived exosomes (M2-exo) in osteogenic differentiation and Hedgehog signaling pathway of mouse bone marrow mesenchymal stem cells (BMSCs) under *in vitro* high-glucose and high-insulin conditions. **Methods**　RAW 264.7 cells were induced toward M2 macrophage polarization and then M2-exo were extracted and identified. Immunofluorescence assay was performed to detect the internalization of M2-exo by BMSCs. BMSCs were divided into the normal control group (Control group), the high-glucose and high-insulin group (HGI group), and the HGI with M2-exo intervention group (HGI+M2e group). BMSCs in the Control group were cultured in osteogenic inductive medium with 5.5 mmol/L glucose, but no insulin or M2-exo. BMSCs in the HGI group were cultured in osteogenic inductive medium with 25 mmol/L glucose and 174 nmol/L insulin. BMSCs in the HGI+M2e group were cultured in the same medium as that of the HGI group, with the additional treatment of 6, 30, 60 μg/mL M2-exo, respectively. After osteogenic induction for 7 days and 14 days, alkaline phosphatase (ALP) staining and alizarin red staining were performed respectively to assess the osteogenic differentiation potential of BMSCs from different groups. In addition, BMSCs in the Control group, HGI group, and HGI+M2e group treated with 30 μg/mL M2-exo were examined with qPCR after osteogenic induction for 14 days and Western blot after osteogenic induction for 21

* 国家自然科学基金资助项目（No. 81771085）、四川省科技厅重点项目（No. 2020YFSY0008）和广东省口腔医学重点实验室开放课题基金项目（No. KF2019120101）资助

△ 通信作者，E-mail：feifeiliyan@163.com

days to assess the osteogenesis and the expression of Hedgehog pathway-related genes and proteins. **Results** M2 macrophage polarization was induced successfully, with highly positive expression of CD206, the M2 polarization surface marker. The M2-exo had the typical structure of round or oval-shaped bilayered-membrane vesicles. The diameter distribution of M2-exo ranged from 50 to 125 nm (accounting for 99.14% of all M2-exo). M2-exo samples showed positive expression of exosomal markers CD9, CD63 and CD81 proteins. Immunofluorescence staining showed that M2-exo were taken up and internalized by BMSCs. After osteogenic induction for 7 days, the ALP activity of BMSCs in the HGI group was lower than that of the Control group. After interventions of 6 μg/mL, 30 μg/mL, and 60 μg/mL M2-exo, the ALP activity of the HGI+M2-exo group was significantly increased compared with that of the HGI group (P<0.05). After osteogenic induction for 14 days, the number of mineralized nodules in the HGI group was lower than that in the Control group, and after intervention, only the HGI+M2e group treated with 30 μg/mL M2-exo showed higher level of mineralization than that in the HGI group (P<0.05). qPCR analysis revealed that the expression levels of the osteogenesis-related genes, including *Runx*2, *Alp* and *Ocn*, and Hedgehog pathway-related genes, including *Gli*1, *Smo* and *Ptch*1, were downregulated in the HGI group, all being lower than those of the Control group to varying degrees, while 30 μg/mL M2-exo treatment could promote the up-regulation of these genes, showing significant difference in comparison with their expression levels in the HGI group (P<0.05). In addition, Western blot analysis showed that the expression of the osteogenesis-related proteins, including RUNX2 and COL1A1, and GLI1, the Hedgehog signaling pathway protein, was down-regulated in the HGI group, while the expression of COL1A1 and GLI1 was up-regulated after 30 μg/mL M2-exo treatment, showing significant difference when compared with that of the HGI group (P<0.05). **Conclusion** High glucose and high insulin had inhibitory effect on the osteogenic differentiation potential of BMSCs. After intervention with M2-exo, the Hedgehog signaling pathway in BMSCs was activated and the osteogenic differentiation potential was enhanced, suggesting that M2-exo might have therapeutic potentials for the treatment of diabetic bone disease.

【Key words】 M2 macrophage Exosome Bone marrow mesenchymal stem cells Diabetes mellitus Hedgehog signaling pathway

2型糖尿病患者往往伴有持续性代偿性高血糖和高胰岛素血症,增加了罹患骨质疏松、骨折及牙周炎等骨疾病的发生风险[1-3]。通过研究其病理机制,积极找寻糖尿病骨病发病后早期的治疗靶点,进而改善患者的预后是关键。研究表明,可通过促进骨微环境中的巨噬细胞M2极化,调节骨免疫,从而达到组织重塑的目的[4-5]。骨髓间充质干细胞(bone marrow mesenchymal stem cells, BMSCs)是成骨细胞的主要来源,直接或间接参与骨修复过程[6]。外泌体是各种生物过程中细胞间通讯的重要信使[7]。目前,M2巨噬细胞外泌体(M2-exo)如何调控高糖高胰岛素条件下的BMSCs尚无报道。Hedgehog信号通路作为骨发育和骨稳态调节的核心,不仅参与BMSCs的成骨分化,还可缓解高糖对BMSCs成骨分化的抑制作用[8-9]。本研究旨在探讨M2-exo对高糖高胰岛素条件下小鼠BMSCs成骨分化及Hedgehog信号通路的影响,为糖尿病骨再生或骨改建的研究提供依据。

1 材料及方法

1.1 主要材料和仪器

胎牛血清(FBS)、高糖DMEM培养基、α-MEM培养基购自美国Gibco公司;葡萄糖、ALP染色试剂盒、BCA试剂盒、氯化十六烷基吡啶、地塞米松、抗坏血酸、RIPA裂解液及PMSF蛋白酶抑制剂购自上海碧云天公司;牛胰岛素、β-甘油磷酸钠、茜素红S染液、DAPI染液购自北京索莱宝公司;PKH67外泌体染料购自上海宇玫博公司;TriZol购自美国Invitrogen公司;RNA逆转录试剂盒、定量PCR试剂盒购自上海翊圣公司;IL-4细胞因子及CD206抗体购自美国ProteinTech公司;CD9、CD63、CD81抗体购自美国BD公司;GLI1抗体购自美国Abcam;RUNX2抗体购自杭州华安生物技术有限公司;COL1A1及β-actin抗体购自上海碧云天公司;辣根过氧化物酶(HRP)标记山羊抗兔二抗及山羊抗小鼠二抗购自美国Affinity公司。实验中使用下列仪器:Optima XPN-100超速离心机(美国Beckman Coulter公司);DMi8倒置荧光显微镜、DMi1倒置相差显微镜(德国Leica公司);SpectraMax iD5酶标仪(美国Molecular Devices公司);Forma 371直热式CO_2细胞培养箱、1 300系列生物安全柜、NanoDrop One C紫外分光光度计、Attune NxT流式细胞仪(美国Thermo公司);纳米流式检测仪(厦门福流公司);HT-7 700透射电镜(日本日立公司);LightCycler 480荧光定量PCR仪(瑞士罗氏公司);ChemiDoc MP化学发光凝胶成像系统(美国Bio-Rad公司)。qPCR引物由上海生工公司合成。

1.2 M2极化诱导细胞培养

复苏冻存于液氮中的小鼠巨噬细胞系RAW 264.7(ATCC TIB-71),细胞培养于含10% FBS的高糖DMEM培养基中。传代后,分别采用10 ng/mL及20 ng/mL细胞因子IL-4诱导其M2极化,48 h后通过流式细胞术及细胞免疫荧光法对M2极化表面标志物CD206进行检测,分析其

极化情况并筛选最佳诱导浓度。细胞荧光染色后，荧光显微镜下随机选取5个不同的视野进行观察，当视野中超过80%的细胞表达CD206时，视为CD206强阳性表达。

1.3　M2巨噬细胞外泌体的提取及鉴定

诱导M2极化后，采用含10%无外泌体FBS（4 ℃，100 000×*g*，离心17 h去除血清中外泌体）的培养基替换原诱导培养基，48 h后收集细胞的培养上清；通过差速超速离心法提取M2-exo：4 ℃，500×*g*，5 min及4 ℃，2 000×*g*，20 min离心去除死细胞及细胞碎片，保留上清液，0.22 μm滤器过滤上清液，10 000×*g*离心30 min除去细胞器后，收集上清；上清液转移至超速离心管中，第1次超速离心（4 ℃，100 000×*g*，2 h）后弃尽上清液，PBS反复冲洗全管内壁，将重悬的外泌体悬液转移至新的超速离心管中；第2次超速离心（4 ℃，100 000×*g*，70 min），弃尽上清液，加入100 μL PBS重悬收集外泌体。经透射电镜（TEM）及纳米流式检测仪对提取的外泌体形态、粒径大小及表面标志蛋白（CD9、CD63、CD81）进行鉴定[10-11]。BCA法测定外泌体总蛋白含量。

1.4　小鼠BMSCs对M2-exo的摄取

复苏冻存于液氮中的小鼠原代BMSCs，培养于含20% FBS的α-MEM培养基中。采用绿色荧光染料PKH67对M2-exo进行染色标记，4 ℃，100 000×*g*超速离心1 h清除残余染料，PBS重悬PKH67标记的M2-exo，将其与第五代BMSCs共培养。4 h后，用40 g/L中性多聚甲醛固定10 min，PBS 洗3 次；加DAPI对细胞核染色，PBS洗涤后荧光显微镜下观察。

1.5　小鼠BMSCs的成骨诱导

将第五代BMSCs以5×10^{4}细胞/孔的密度接种于24孔板，待细胞融合至约80%，使用成骨诱导培养基（含10 mmol/L β-甘油磷酸钠、10^{-8} mol/L地塞米松、50 μg/mL抗坏血酸）替换原培养基。实验组细胞培养于含25 mmol/L葡萄糖及174 nmol/L胰岛素的成骨诱导培养基，并分别采用不同质量浓度的M2-exo进行干预。根据文献[12-14]，将高糖高胰岛素组（high glucose and insulin group，HGI组）M2-exo的质量浓度设置为0，HGI+M2-exo组的M2-exo的质量浓度设置为6、30、60 μg/mL。此外，将培养于不含胰岛素、不含M2-exo，葡萄糖浓度为5.5 mmol/L的成骨诱导培养基的BMSCs作为正常对照（Control）组。

在成骨诱导7 d后，进行ALP染色并采用Image J软件分析ALP阳性面积所占百分比[15]，检测早期成骨能力。在成骨诱导液培养14 d后，采用40 mmol/L茜素红S溶液（pH4.2）进行染色，PBS漂洗后观察矿化情况并拍照。使用100 mmol/L氯化十六烷基吡啶溶解矿化结节，吸取100 μL溶液至96孔板，通过酶标仪测定405 nm光谱下各孔吸光度值OD_{405nm}，对细胞矿化结节进行定量分析。

1.6　BMSCs中基因和蛋白的检测

将第五代BMSCs以1×10^{6}细胞/孔的密度接种于6孔板中，当细胞融合至约80%时，按1.5的培养基成分分为3组：Control组、HGI组、HGI+M2e组，其中HGI+M2e组仅取30 μg/mL M2-exo的浓度组进行实验。成骨诱导14 d后检测相关基因；成骨诱导21 d后检测相关蛋白。

1.6.1　qPCR检测成骨相关基因及Hedgehog通路相关基因　成骨诱导14 d后提取细胞总RNA，紫外分光光度计检测纯度及浓度。采用逆转录试剂盒将RNA转录成cDNA。根据qPCR试剂盒说明书，检测成骨相关基因Runt-related transcription factor 2 (*Runx*2)、Alkaline phosphatase (*Alp*)和Osteocalcin (*Ocn*)及Hedgehog通路相关基因GLI-Kruppel family member GLI 1 (*Gli*1)、smoothened, frizzled class receptor (*Smo*)和patched 1 (*Ptch*1)的表达变化。以*β-actin*为内参，采用$2^{-\Delta\Delta Ct}$法分析各基因表达水平。引物序列见表1。

1.6.2　Western Blot检测成骨相关蛋白RUNX2、COL1A1及Hedgehog通路蛋白GLI1的表达变化　成骨诱导21 d后，收集各组细胞，加入RIPA裂解液（含PMSF）提取总蛋白。BCA法测定蛋白浓度。采用Bio-Rad系统对蛋白样品进行SDS-PAGE电泳，恒流200 mA冰浴将蛋白转印至0.22 μm PVDF膜（Millipore），5% 脱脂牛奶封闭2 h后，加入一抗RUNX2（1∶1 000）、COL1A1（1∶1 000）、GLI1

表 1　实时荧光定量PCR引物序列

Table 1　Primer sequences used for real-time PCR analysis

Gene	Forward primer (5′ to 3′)	Reverse primer (5′ to 3′)	Product length/bp
*Runx*2	ATGCTTCATTCGCCTCACAAA	GCACTCACTGACTCGGTTGG	146
Alp	CCAACTCTTTTGTGCCAGAGA	GGCTACATTGGTGTTGAGCTTTT	110
Ocn	CTGACCTCACAGATCCCAAGC	TGGTCTGATAGCTCGTCACAAG	187
*Gli*1	CCAAGCCAACTTTATGTCAGGG	AGCCCGCTTCTTTGTTAATTTGA	130
Smo	GAGCGTAGCTTCCGGGACTA	CTGGGCCGATTCTTGATCTCA	101
*Ptch*1	AAAGAACTGCGGCAAGTTTTTG	CTTCTCCTATCTTCTGACGGGT	164
β-actin	GGCTGTATTCCCCTCCATCG	CCAGTTGGTAACAATGCCATGT	154

*Runx*2: Runt-related transcription factor 2; *Alp*: Alkaline phosphatase; *Ocn*: Osteocalcin; *Gli*1: GLI-Kruppel family member GLI 1; *Smo*: Smoothened, frizzled class receptor; *Ptch*1: Patched 1.

(1∶1 000)及β-actin(1∶1 000)4 ℃孵育过夜。次日采用TBST漂洗后,加入HRP标记的山羊抗兔/山羊抗小鼠IgG二抗(1∶5 000),室温孵育1.5 h。漂洗后,滴加化学发光(ECL)显影液,通过ChemiDoc MP化学发光凝胶成像系统获取图像。以β-actin为内参,使用Image J软件对灰度值进行量化和归一化分析。

1.7 统计学方法

各实验重复3次,重复性好。正态分布的计量资料以$\bar{x}\pm s$表示,采用单因素方差分析进行多组间比较,采用Tukey's HSD法进行两两比较。P<0.05为差异有统计学意义。

2 结果

2.1 RAW 264.7成功被诱导为M2巨噬细胞

如图1所示,诱导前细胞状态良好,多为透亮的圆形,贴壁生长;10 ng/mL及20 ng/mL 的IL-4诱导48 h后细胞触角伸长(图1A)。流式细胞术结果显示,约80%的细胞可被10 ng/mL及20 ng/mL的IL-4诱导为CD206$^+$细胞,且2种浓度的诱导效果无显著差异(P>0.05)(图1B)。进一步对采用10 ng/mL IL-4诱导的细胞进行免疫荧光染色,结果显示,与未诱导组相比,诱导组细胞呈CD206强阳性(图1C)。因此,后续实验选取浓度为10 ng/mL的IL-4进行诱导。

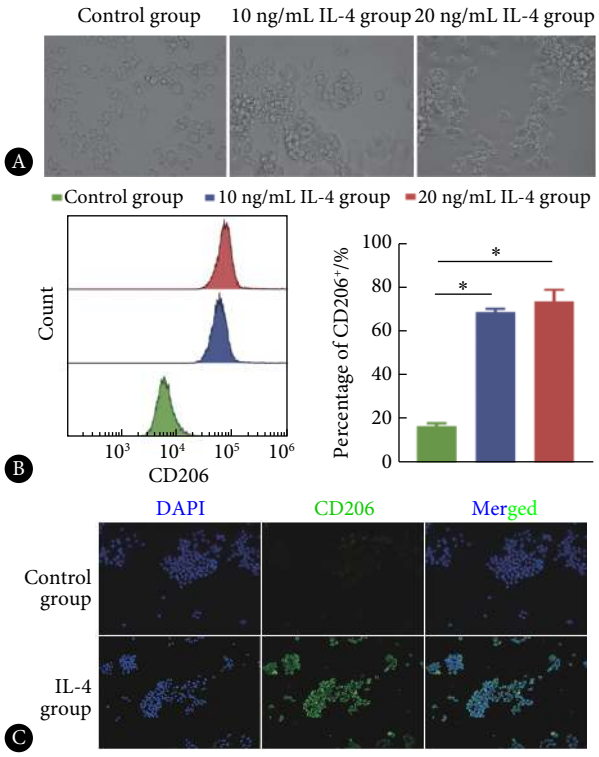

图 1 RAW264.7极化为M2巨噬细胞

Fig 1 RAW264.7 macrophage cells were induced for polarization toward M2 macrophage

A: Morphology of RAW264.7 macrophage cells before and after 10 ng/mL and 20 ng/mL IL-4 treatment (×100); B: Flow cytometry of M2 phenotype marker CD206 in RAW264.7 induced by different concentrations of IL-4, *P<0.05, n=3; C: Immunofluorescence staining of CD206$^+$ cells (×100).

2.2 M2-exo鉴定

透射电子显微镜对外泌体进行形态学观察,可见M2-exo呈类圆形双层膜性囊泡样结构(图2A);纳米流式

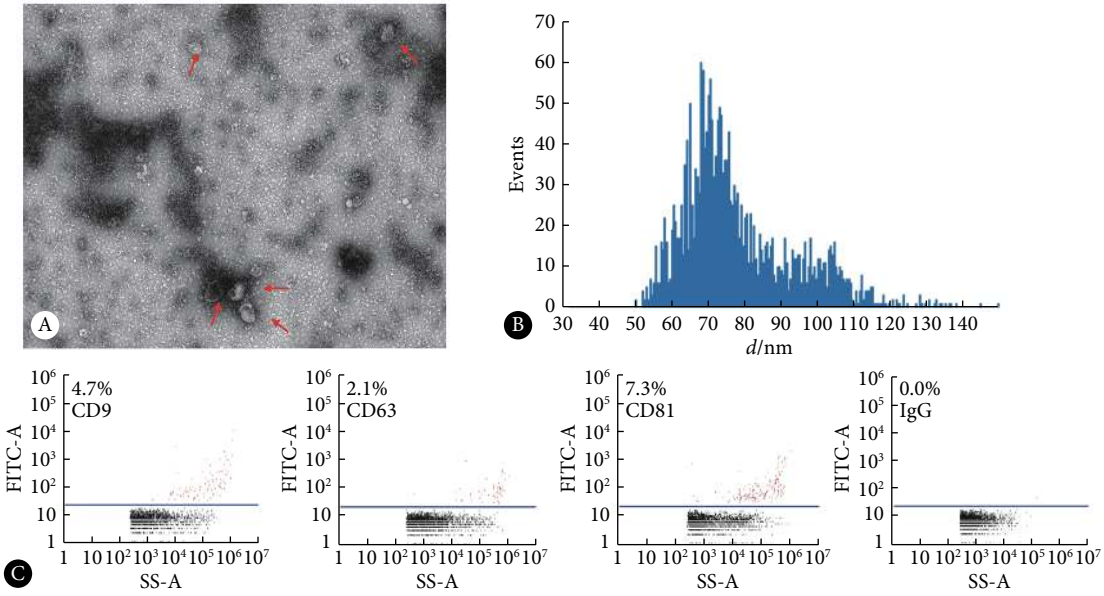

图 2 M2巨噬细胞外泌体的鉴定

Fig 2 Identification of exosomes secreted by M2 macrophages (M2-exo)

A: M2-exo was examined by electron transmission electron microscopy (TEM)(×10 000); red arrows indicate typical cup-shaped exosomes; B: M2-exo particle size distribution was determined by nano-flow cytometry (NanoFCM); C: Exosomal markers (CD9, CD63 and CD81) were determined by NanoFCM; positive particles are shown above the blue lines.

技术检测发现, M2-exo粒径主峰值为68.25 nm, 平均粒径78.35 nm, 主要分布于50 ~ 125 nm(占总粒子数的99.14%), 且提取浓度为2.14 ×10^{10} Particles/mL(图2B)。此外, 外泌体标志蛋白CD9、CD63和CD81在M2-exo中呈阳性表达, 同型对照IgG为阴性(图2C)。

2.3　M2-exo可被小鼠BMSCs摄取

见图3。将M2-exo与BMSCs 共培养4 h 后, 蓝色荧光标记的BMSCs细胞核附近出现绿色荧光标记的外泌体, 表明M2-exo被BMSCs成功摄取进入胞内且分布在细胞核周围。

2.4　M2-exo逆转ALP活性

成骨诱导7 d后(图4), HGI组ALP表达低于Control组(P<0.05)。与HGI组相比, 6 μg/mL、30 μg/mL及60 μg/mL M2-exo干预后均可增加ALP染色阳性面积(P<0.05)。

2.5　M2-exo促进矿化结节形成

茜素红染色及矿化定量结果(图5)提示, HGI组BMSCs的矿化结节数量较Control组减少(P<0.05), 而经M2-exo干预可提高矿化结节形成能力, 逆转高糖高胰岛素对BMSCs成骨的抑制作用。其中30 μg/mL M2-exo作用后与HGI组相比, 差异有统计学意义(P<0.05), 与Control组的水平相当(P>0.05); 6 μg/mL M2-exo和60 μg/mLM2-exo也可促进矿化结节形成, 但与HGI组相比, 差异无统计学意义(P>0.05)。

2.6　M2-exo激活Hedgehog信号通路

qPCR检测结果(图6A)显示, 成骨诱导14 d后, 与Control组相比, HGI组Hedgehog通路相关基因*Gli*1、*Smo*及*Ptch*1的表达总体呈现下降趋势; 而与HGI组相比, HGI-M2e组以上基因不同程度上调, 其中*Gli*1上调最为显著(P<0.05)。Western blot 检测结果(图6B)显示, 成骨诱导21 d后, 与Control组相比, HGI组Hedgehog信号通路关键蛋白GLI1的表达显著下调(P<0.05); 而HGI-M2e组GLI1表达高于HGI组(P<0.05), 达到与Control组相当的水平。

2.7　M2-exo促进成骨分化

qPCR检测结果(图7A)显示, 成骨诱导14 d后, 与Control组相比, HGI组成骨分化相关基因*Runx*2、*Alp*及*Ocn* mRNA水平均显著下调(P<0.05); 相较于HGI组, HGI-M2e组以上基因不同程度上调, 其中*Alp*及*Ocn*上调最为显著(P<0.05)。Western blot 检测结果(图7B)显示, 成骨诱导21 d后, HGI组细胞早期矿化指标RUNX2、晚期矿化指标COL1A1的表达均低于Control组(P<0.05); HGI-M2e组的COL1A1表达高于HGI组(P<0.05), 达到与Control组相当的水平。

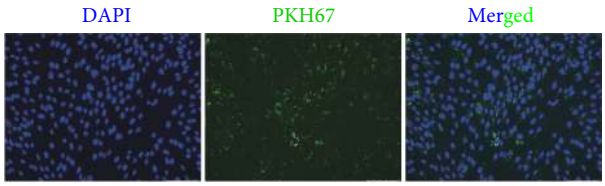

图 3　小鼠骨髓间充质干细胞对M2巨噬细胞外泌体的摄取。　免疫荧光染色×100

Fig 3　M2 macrophage exosomes were taken up by mouse BMSCs. Immnunofluorescence staining ×100

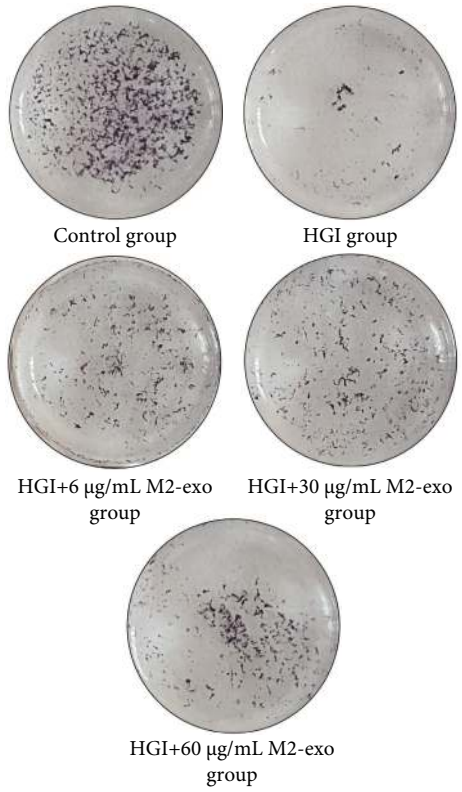

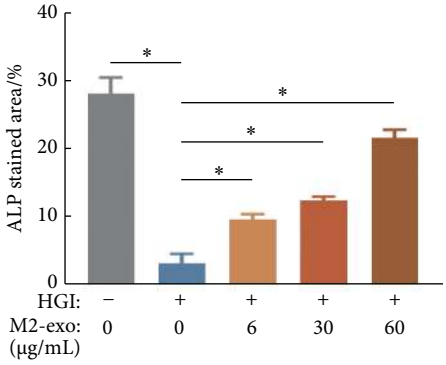

图 4　各组BMSCs的ALP染色比较

Fig 4　The ALP staining of BMSCs in different groups

The representative ALP staining (×5) of BMSCs after 7 days of osteogenic induction, and ALP-positive area was calculated as ([stained area/disk area] × 100%) using Image J software (n=3). *P<0.05.

3　讨论

2型糖尿病患者常继发骨骼疾病, 其进展被认为与血

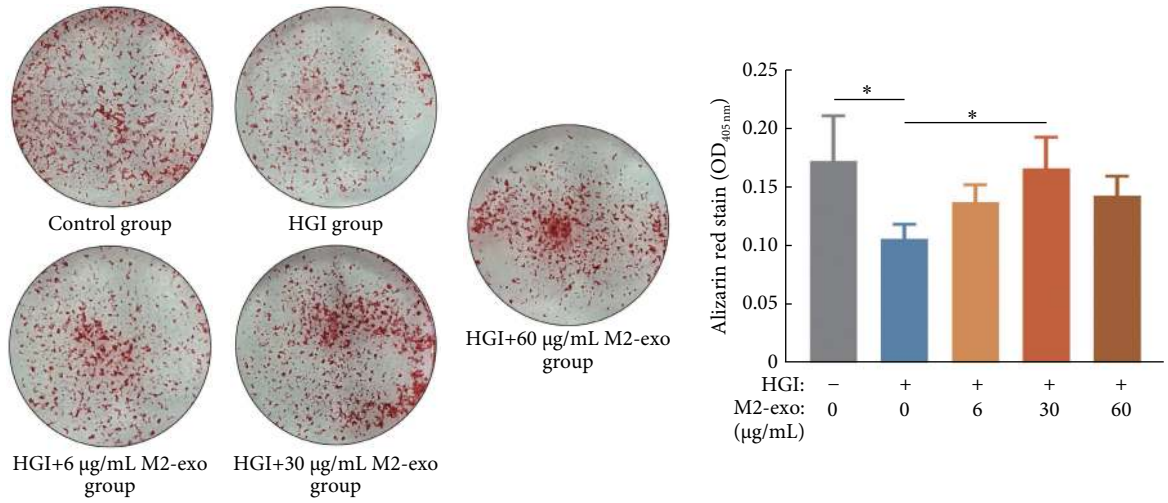

图 5 茜素红染色（×5）及定量分析检测M2-exo对BMSCs矿化结节形成的影响

Fig 5 The alizarin red S staining (×5) and quantitative analysis of the effect of M2-exo on the formation of mineralized nodules in BMSCs

*P<0.05, n=3.

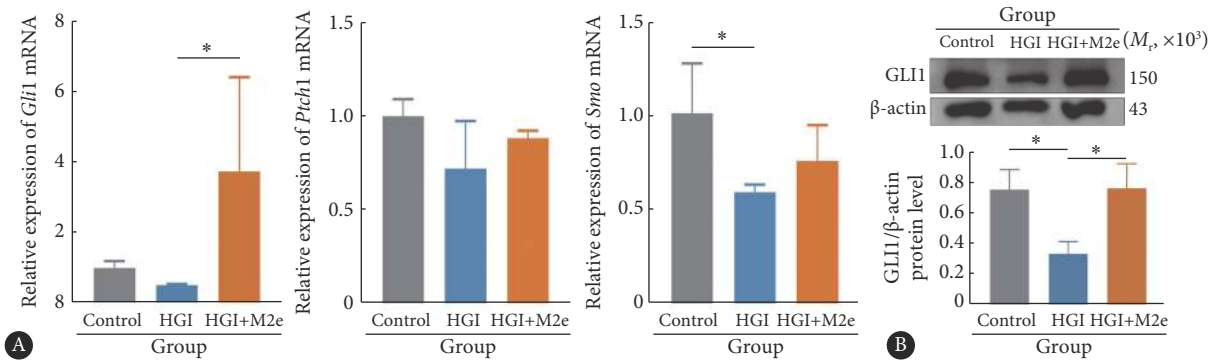

图 6 Hedgehog通路相关基因及蛋白的表达

Fig 6 The expression of Hedgehog signaling-related genes and protein

A: The mRNA level of *Gli*1, *Smo* and *Ptch*1 mRNA were determined by qPCR; B: The protein level of GLI1 was examined with Western blot. *P<0.05, n=3.

糖和胰岛素水平的改变有关。糖尿病高糖高胰岛素微环境中BMSCs的分化、增殖及功能障碍可能是导致糖尿病相关性骨丢失的重要因素[16-17]。越来越多的研究表明，高糖高胰岛素会抑制BMSCs的成骨能力[18-19]。而骨组织的再生及重建主要依赖于干细胞的增殖及分化能力，因此逆转高糖高胰岛素微环境对BMSCs的抑制作用非常关键。

ALP 是公认的矿化早期标志物，但它很难准确预测成骨分化晚期的变化，因此我们还检测了OCN及COL1A1这类成骨晚期标志物。Runx2作为成骨分化过程中的重要核转录因子，通过多种途径参与调节骨代谢，对骨组织的形成和重建十分重要[20]。本研究采用高糖高胰岛素培养基体外模拟2型糖尿病骨微环境，发现小鼠BMSCs成骨相关基因（*Alp*、*Runx*2和*Ocn*）及蛋白（RUNX2和COL1A1）的表达受抑制，ALP活性有所降低，矿化结节形成能力显著下降，均表明高糖高胰岛素微环境不利于成骨，这与既往研究基本一致[18-19]。

作为细胞间通讯的重要媒介，外泌体近年来亦是骨再生领域的研究热点。外泌体的分离提取技术日渐成熟，其主流的提取方法包括：差速超速离心法、密度梯度离心法、超滤膜过滤法、尺寸排阻色谱法等[21]。而差速超速离心是目前受到广泛认可的外泌体提取方法，能获得纯度最高的外泌体[10]。本研究选取这一方法制备了M2极化巨噬细胞外泌体，并综合利用透射电镜及纳米流式对外泌体的形态、粒径及表面蛋白进行了鉴定，与传统的Western blot及纳米颗粒跟踪分析（NTA）技术相比，纳米流式灵敏度高且可以实现在单颗粒水平上对外泌体逐个计数，具有显著的优势[10]。本研究提取的M2-exo具有促进高糖高胰岛素微环境中的BMSCs的成骨分化的能力，表明其在糖尿病骨病治疗中颇具潜力，与以往的文献报道基本一致[12, 22-23]。此外，我们发现M2-exo在中、低浓度下可以促进高糖高胰岛素环境中BMSCs的矿化结节形成；而其在高浓度下的促进作用反而下降，这可能与既往

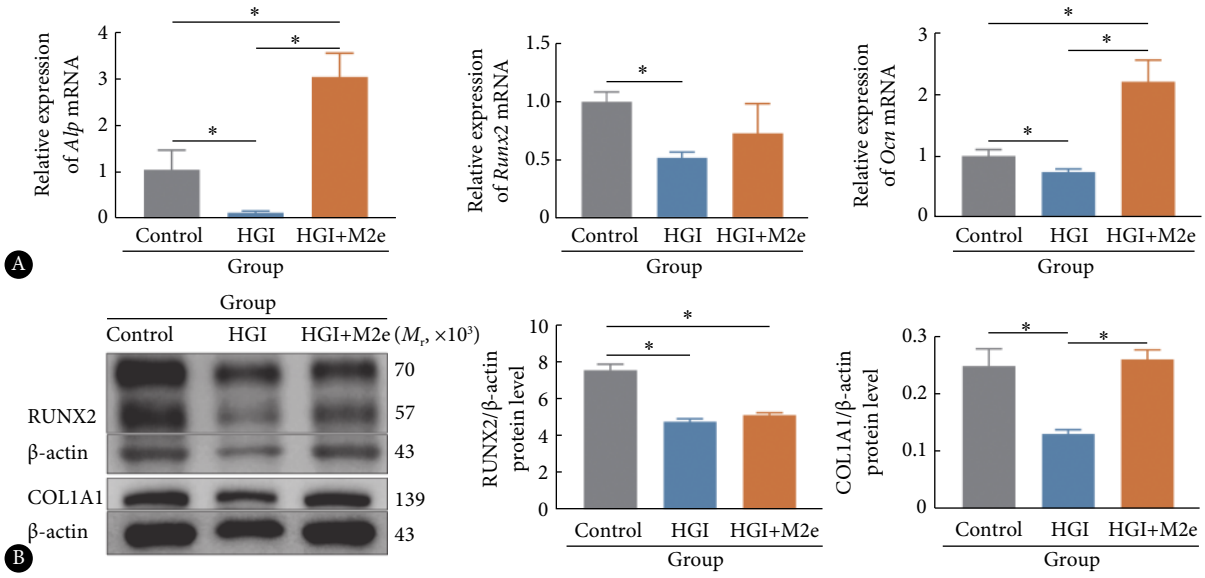

图 7 成骨分化相关基因及蛋白的表达

Fig 7 The expression of osteogenic differentiation related genes and proteins

A: The mRNA level of *Alp*, *Runx*2 and *Ocn* mRNA were determined by qPCR; B: The protein level of RUNX2 and COL1A1 were examined with Western blot. **P*<0.05, *n*=3.

报道的细胞外囊泡所具有的"双相效应"有关[14, 24-25]，因此在外泌体的实际应用中应注意最佳剂量筛选。

Hedgehog信号通路的激活是通过Hedgehog配体与跨膜受体Patched1（PTCH1）结合，继而解除其对Smoothened（SMO）的抑制作用而实现。激活的SMO在初级纤毛激活GLI转录因子家族[26]。GLI转录因子（主要是GLI1和GLI2）随后进入细胞核，激活下游靶基因的表达，其中包括Hedgehog通路组件本身（PTCH1、GLI1等）的转录反馈调节[27]。在体外研究中，Hedgehog信号通路可通过激活下游关键分子SMO及GLI1促进BMSCs成骨分化；而该信号通路的中断会导致骨缺损。以往的研究表明，暴露于高糖环境下可抑制BMSCs的Sonic hedgehog信号通路，而通过添加通路关键蛋白Shh等手段激活信号通路，则可抵消高糖环境对成骨分化的抑制作用[9]。本研究发现，经过M2-exo干预后，在成骨诱导14 d时*Gli*1 mRNA的表达水平显著上调，同时*Ptch*1及*Smo*有上调趋势；而成骨诱导21 d时，GLI1蛋白表达水平显著上调。我们的数据提示，高糖高胰岛素微环境可抑制BMSCs的Hedgehog信号通路，而经过M2-exo干预后，该通路得到了修复，同时成骨分化的抑制也得到改善。

综上所述，本研究表明M2-exo可激活高糖高胰岛素微环境中BMSCs的Hedgehog信号通路并促进成骨分化，表明其可作为糖尿病骨免疫稳态重塑的新途径。就本研究目前的结果而言，我们仅能证明在M2-exo的干预下，高糖高胰岛素微环境中BMSCs的Hedgehog信号通路被激活，且BMSCs的成骨分化作用得到提高，至于M2-exo是否通过调控该信号通路从而恢复BMSCs的成骨分化能力，我们后续将通过进一步体内实验进行深入探讨。

*　　*　　*

利益冲突　所有作者均声明不存在利益冲突

参　考　文　献

[1] RODEN M, SHULMAN G I. The integrative biology of type 2 diabetes. Nature, 2019, 576(7785): 51–60.

[2] LALLA E, PAPAPANOU P N. Diabetes mellitus and periodontitis: A tale of two common interrelated diseases. Nat Rev Endocrinol, 2011, 7(12): 738–748.

[3] NAPOLI N, CHANDRAN M, PIERROZ D D, *et al*. Mechanisms of diabetes mellitus-induced bone fragility. Nat Rev Endocrinol, 2017, 13(4): 208–219.

[4] RAIMONDO T M, MOONEY D J. Functional muscle recovery with nanoparticle-directed M2 macrophage polarization in mice. Proc Natl Acad Sci U S A, 2018, 115(42): 10648–10653.

[5] YIN C, ZHAO Q, LI W, *et al*. Biomimetic anti-inflammatory nanocapsule serves as a cytokine blocker and M2 polarization inducer for bone tissue repair. Acta Biomater, 2020, 102: 416–426[2021-09-01]. https://doi.org/10.1016/j.actbio.2019.11.025.

[6] PITTENGER M F, DISCHER D E, PéAULT B M, *et al*. Mesenchymal stem cell perspective: Cell biology to clinical progress. NPJ Regen Med, 2019, 4(1): 22[2021-09-01]. https://doi.org/10.1038/s41536-019-0083-6.

[7] LIU J, LI D, WU X, *et al*. Bone-derived exosomes. Curr Opin Pharmacol, 2017, 34: 64-69[2021-09-01]. https://doi.org/10.1016/j.

coph.2017.08.008.

[8] LV W T, DU D H, GAO R J, *et al*. Regulation of Hedgehog signaling offers a novel perspective for bone homeostasis disorder treatment. Int J Mol Sci, 2019, 20(16):3981[2021-09-01]. https://doi.org/10.3390/ijms20163981.

[9] GUAN C-C, YAN M, JIANG X-Q, *et al*. Sonic Hedgehog alleviates the inhibitory effects of high glucose on the osteoblastic differentiation of bone marrow stromal cells. Bone, 2009, 45(6): 1146–1152.

[10] TIAN Y, GONG M, HU Y, *et al*. Quality and efficiency assessment of six extracellular vesicle isolation methods by nano-flow cytometry. J Extracell Vesicles, 2020, 9(1): 1697028[2021-09-01]. https://doi.org/10.1080/20013078.2019.1697028.

[11] TIAN Y, MA L, GONG M, *et al*. Protein profiling and sizing of extracellular vesicles from colorectal cancer patients via flow cytometry. ACS Nano, 2018, 12(1): 671–680.

[12] XIA Y, HE X T, XU X Y, *et al*. Exosomes derived from M0, M1 and M2 macrophages exert distinct influences on the proliferation and differentiation of mesenchymal stem cells. Peer J, 2020, 8: e8970[2021-09-01]. https://doi.org/10.7717/peerj.8970.

[13] ZHANG S, YANG Y, JIA S, *et al*. Exosome-like vesicles derived from Hertwig's epithelial root sheath cells promote the regeneration of dentin-pulp tissue. Theranostics, 2020, 10(13): 5914–5931.

[14] WEI J, SONG Y, DU Z, *et al*. Exosomes derived from human exfoliated deciduous teeth ameliorate adult bone loss in mice through promoting osteogenesis. J Mol Histol, 2020, 51(4): 455–466.

[15] CHIARELLA E, ALOISIO A, SCICCHITANO S, *et al*. ZNF521 represses osteoblastic differentiation in human adipose-derived stem cells. Int J Mol Sci, 2018, 19(12): 4095[2021-09-01]. https://doi.org/10.3390/ijms19124095.

[16] SARGENT J. Diabetes: Functional impairment of bone marrow progenitor cells in diabetes mellitus. Nat Rev Endocrinol, 2014, 10(7): 379[2021-09-01]. https://doi.org/10.1038/nrendo.2014.66.

[17] DENG X, XU M, SHEN M, *et al*. Effects of type 2 diabetic serum on proliferation and osteogenic differentiation of mesenchymal stem cells. J Diabetes Res, 2018, 2018: 5765478[2021-09-01]. https://doi.org/10.1155/2018/5765478.

[18] ZHANG P, ZHANG H, LIN J, *et al*. Insulin impedes osteogenesis of BMSCs by inhibiting autophagy and promoting premature senescence via the TGF-β1 pathway. Aging, 2020, 12(3): 2084–2100.

[19] CAO B, LIU N, WANG W. High glucose prevents osteogenic differentiation of mesenchymal stem cells via lncRNA AK028326/CXCL13 pathway. Biomed Pharmacother, 2016, 84: 544–551[2021-09-01]. https://doi.org/10.1016/j.biopha.2016.09.058.

[20] QIN X, JIANG Q, KOMORI H, *et al*. Runt-related transcription factor-2 (Runx2) is required for bone matrix protein gene expression in committed osteoblasts in mice. J Bone Miner Res, 2021, 36(10): 2081–2095.

[21] CRESCITELLI R, LÄSSER C, LÖTVALL J. Isolation and characterization of extracellular vesicle subpopulations from tissues. Nat Protoc, 2021, 16(3): 1548–1580.

[22] LI Z, WANG Y, LI S, *et al*. Exosomes derived from M2 macrophages facilitate osteogenesis and reduce adipogenesis of BMSCs. Front Endocrinol (Lausanne), 2021, 12: 680328[2021-09-01]. https://doi.org/10.3389/fendo.2021.680328.

[23] XIONG Y, CHEN L, YAN C, *et al*. M2 macrophagy-derived exosomal miRNA-5106 induces bone mesenchymal stem cells towards osteoblastic fate by targeting salt-inducible kinase 2 and 3. J Nanobiotechnol, 2020, 18(1): 66[2021-09-01]. https://doi.org/10.1186/s12951-020-00622-5.

[24] LACROIX R, SABATIER F, MIALHE A, *et al*. Activation of plasminogen into plasmin at the surface of endothelial microparticles: A mechanism that modulates angiogenic properties of endothelial progenitor cells *in vitro*. Blood, 2007, 110(7): 2432–2439.

[25] HELLWINKEL J E, REDZIC J S, HARLAND T A, *et al*. Glioma-derived extracellular vesicles selectively suppress immune responses. Neuro Oncol, 2016, 18(4): 497–506.

[26] PAK E, SEGAL ROSALIND A. Hedgehog signal transduction: Key players, oncogenic drivers, and cancer therapy. Dev Cell, 2016, 38(4): 333–344.

[27] BRISCOE J, THÉROND P P. The mechanisms of Hedgehog signalling and its roles in development and disease. Nat Rev Mol Cell Biol, 2013, 14(7): 416–429.

（2021－09－20收稿, 2021－12－13修回）

编辑 吕 熙